Josephson Junction as a Detector of Poissonian Charge Injection

J. P. Pekola

Low Temperature Laboratory, Helsinki University of Technology, P.O. Box 3500, 02015 HUT, Finland

(Received 24 March 2004; published 10 November 2004)

We propose a scheme of measuring the non-Gaussian character of noise by a hysteretic Josephson junction in the macroscopic quantum tunneling regime. We model the detector as an (under)damped LC resonator. It transforms Poissonian charge injection into current through the detector, which samples the injection statistics over a floating time window of length $\sim Q/\omega_J$, where Q is the quality factor of the resonator and ω_J its resonance frequency. This scheme ought to reveal the Poisson character of charge injection in a detector with realistic parameters.

DOI: 10.1103/PhysRevLett.93.206601 PACS numbers: 72.70.+m, 05.40.–a, 73.23.–b

Presently there is considerable effort on characterizing and measuring the statistics of electrical current and the non-Gaussian nature of its fluctuations in mesoscopic conductors [1,2]. The discrete nature of charge injection, e.g., in tunnel junctions, with typically Poissonian statistics can be revealed by studying not only the average current $\langle I \rangle$ and its variance $\langle \delta I^2 \rangle$, unlike in the case of normally distributed current, but higher moments also, most notably the third (central) moment $\langle \delta I^3 \rangle$. Normally these higher moments introduce very small signals and the filtering requirements are strict, because of which it is very hard to measure them (see, e.g., [3,4]). There is, however, one recent experiment which succeeded in demonstrating the existence of the nonvanishing third moment in transport through a nonsuperconducting tunnel junction [4], and which thereby provided valuable information on, e.g., the distribution of the conduction channels of the sample. The measurement required very long averaging times. Therefore, alternative techniques to collect more information, and perhaps eventually to determine further higher moments, are definitely needed. Already in 1994 Lesovik proposed to probe non-Gaussian fluctuations via frequency drift in Josephson generation [5]. More recently Tobiska and Nazarov [6] introduced an overdamped Josephson tunnel junction (array) as a threshold detector to measure such full counting statistics (FCS) making use of rare over-the-barrier jumps arising from current fluctuations. The nearby on-chip detector is a definite benefit of this proposal due to its natural high bandwidth. Yet they considered the limit where tunneling is perfectly suppressed whereby the setup becomes experimentally less accessible. In our proposal we consider an underdamped single Josephson junction (or a dc-SQUID) in the macroscopic quantum tunneling (MQT) limit. We demonstrate that the experimental complications of the proposal [6], e.g., the need of a multijunction Josephson junction array, and the fact that the escape threshold is more difficult to measure in an overdamped junction, are overcome in our scheme, and show that the effect of higher moments is pronounced using a threshold detector with parameters deduced from earlier MQT experiments (see, e.g., Ref. [7]).

We discuss a simplified model where charges are injected according to Poisson statistics [8] on a Josephson junction, which in turn is described by a damped harmonic oscillator [LCR, or a linearized resistively and capacitively shunted junction (RCSJ) model]. We show how this environment performs a conversion from discrete (charge) statistics into continuous (current) statistics. The proposed scheme is sketched in Fig. 1. The two injecting lines carry currents I_1 and I_2, respectively. I_1 is generated by a voltage bias across the scatterer (for example, a tunnel junction), and I_2 runs in a directly connected line to be discussed below. We neglect the influence of the transmission line connecting the injecting lines and the measuring Josephson junction. Capacitance of the injecting junction can be included in the RCSJ capacitance, and similarly the additional injection line (I_2) and the connection to the voltage amplifier can be modeled as a parallel inductance, which may reduce the resolution of

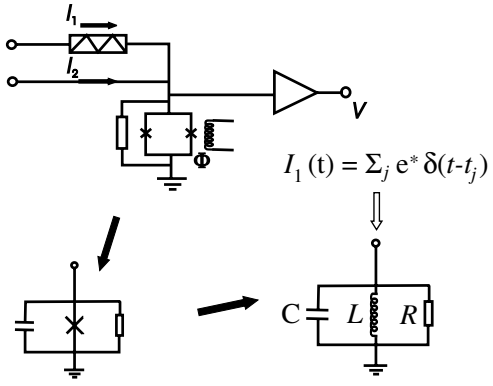

FIG. 1. The scheme of the threshold measurement and the model. The current through the Josephson junction (or a dc-SQUID) is determined by those through the scatterer (I_1) and the ideal bias line (I_2), respectively. Switching to the normal state of the Josephson junction is signaled by a nonzero voltage V at the output of the amplifier. The resonator model and the charge injection are discussed in the text.

 © 2004 The American Physical Society

the detector as will be discussed at the end. For practical implementations we depict the detector as a dc-SQUID with critical current tunable by magnetic flux Φ.

The detector is driven by elementary charges e^* "dropped" on the LCR resonator at time instants t_j [9]. Therefore, each event poses an elementary current $e^*\delta(t-t_j)$ into the resonator such that $I_1(t)=\sum_j e^*\delta(t-t_j)$ as illustrated in Fig. 1. Here $\delta(t)$ is the Dirac delta function. (Alternatively we could consider a voltage step of height e^*/C at each instant t_j.) Our task is to evaluate the current I and its moments through the junction (inductor L). The elementary current $i(t,t_j)$ through the Josephson junction at the time instant t is given in the case of an underdamped resonator (quality factor $Q\equiv R/\sqrt{L/C}>1/2$) by

$$i(t,t_j)=e^*\omega_J\left(1-\frac{1}{4Q^2}\right)^{-1/2}\exp\left[-\frac{1}{2Q}\omega_J(t-t_j)\right]\times\sin\left[\left(1-\frac{1}{4Q^2}\right)^{1/2}\omega_J(t-t_j)\right]\theta(t-t_j). \quad (1)$$

Here, $\omega_J=(LC)^{-1/2}$ is the plasma frequency of the junction and $\theta(t)$ is the Heaviside step function. Analogous results for overdamped case ($Q<1/2$) exist, but they are not considered explicitly here, since the detector is assumed to *switch* from supercurrent state to resistive state. Therefore we assume $Q>1/2$ in what follows unless otherwise noted. It is interesting to see some properties of these elementary oscillations. At the time instant t_j all charge e^* is stored in the capacitor C, whereafter it performs damped oscillations at (angular) frequency ω_J. On integrating $i_j(t)$ one finds a consistent result: $\int_{-\infty}^{+\infty} i(t,t_j)=e^*$.

$I_1(t)$ induces current $I(t)$ through the Josephson junction that can be expressed, on the basis of linearity, as the sum of the elementary currents of Eq. (1):

$$I(t)=\sum_j i(t,t_j), \quad (2)$$

where now the time instants t_j are perfectly uncorrelated. One can numerically simulate the current following the Poisson principle: divide time into very small intervals δt and set the probability $p\ll 1$ for one charge to tunnel during this interval. No multiple events in any of the δt intervals are allowed. The average current $\bar{I}$, p, and δt are related through $\bar{I}=pe^*/\delta t$. Figure 2 illustrates results of simulation with two different values of Q, the time unit is ω_J^{-1}, and $\bar{I}=100$, in units $e^*\omega_J$. The initial rise and oscillations are due to the fact that the injection of charges is suddenly initiated at $t=0$. At larger values of Q the junction tends to oscillate at (angular) frequency ω_J, but it is driven by random events and thereby dephased.

Let us next consider the various moments of $I(t)$. We take a long enough time interval τ such that the interesting instant t at which we want to evaluate the moments of current satisfies $t\le\tau$. Now we consider different ensembles of instants t_j, such that N charges are injected within τ, and then weight all these configurations by the Poisson probability $P_{\mathrm{Poisson}}(N)$. Since all the $j=1,\ldots,N$ events are uncorrelated and evenly distributed over $0\le t_j\le\tau$, we may write for the nth moment of $I(t)$:

$$\langle I^n(t)\rangle=\sum_{N=1}^{\infty}P_{\mathrm{Poisson}}(N)\tau^{-N}\int_0^\tau\int_0^\tau\cdots\int_0^\tau dt_1dt_2\cdots dt_N\left[\sum_{j=1}^{N}i(t,t_j)\right]^n. \quad (3)$$

It is straightforward to integrate for $\langle I^n(t)\rangle$ using $i(t,t_j)$ of Eq. (1). Below we summarize results for the three lowest moments of $I(t)$. The average current reads

$$\langle I(t)\rangle=\bar{I}\left\{1-\exp\left(-\frac{\omega_J}{2Q}t\right)\left[\cos\left(\sqrt{1-\frac{1}{4Q^2}}\omega_Jt\right)+\frac{1}{\sqrt{1-\frac{1}{4Q^2}}}\sin\left(\sqrt{1-\frac{1}{4Q^2}}\omega_Jt\right)\right]\right\}. \quad (4)$$

Here we have identified $\bar{I}=e^*\langle N\rangle/\tau\equiv\frac{e^*}{\tau}\times\sum_{N=1}^{\infty}NP_{\mathrm{Poisson}}(N)$, which is the asymptotic value of $\langle I(t)\rangle$ on $t\to\infty$. The thick lines in Fig. 2 show the result of $\langle I(t)\rangle$ using Eq. (4), which indeed seem to follow the mean of the simulated curves. In what follows, we drop out the argument t, and consider only results after the initial transient, i.e., $t\gg 2Q/\omega_J$. The second raw moment reads $\langle I^2\rangle=\frac{Qe^*\omega_J}{2}\bar{I}+\frac{e^{*2}}{\tau^2}\langle N(N-1)\rangle$, where $\langle N(N-1)\rangle\equiv\sum_{N=1}^{\infty}N(N-1)P_{\mathrm{Poisson}}(N)$. The more interesting second central moment, the variance $\langle\delta I^2\rangle\equiv\langle(I-\langle I\rangle)^2\rangle$, then reduces to

$$\langle\delta I^2\rangle=\frac{Qe^*\omega_J}{2}\bar{I}. \quad (5)$$

After a straightforward derivation we similarly obtain the third central moment, $\langle\delta I^3\rangle\equiv\langle(I-\langle I\rangle)^3\rangle$, reading

$$\langle\delta I^3\rangle=\frac{2}{3(1+2/Q^2)}(e^*\omega_J)^2\bar{I}. \quad (6)$$

According to Eq. (5), the shot noise of the injecting junction, $2e^*\bar{I}$, is amplified by the quality factor of the resonator over the band whose width is $\sim\omega_J$, the (maximum) response frequency of the detector. A measure of the non-Gaussian character of the current distribution is its skewness, defined as $S=\langle\delta I^3\rangle/\langle\delta I^2\rangle^{3/2}$, which, according to Eqs. (5) and (6), reads

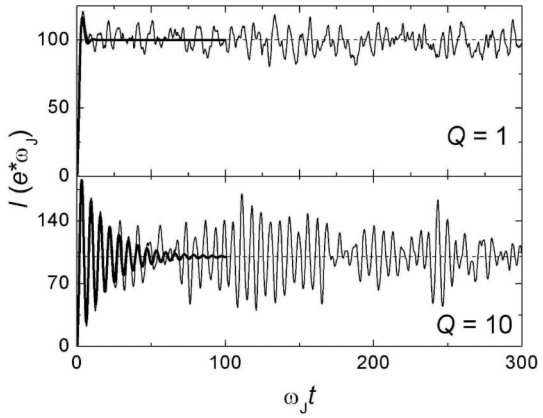

FIG. 2. Simulated $I(t)$ (thin solid lines) with the following parameters: $\bar{I} = 100$ and $p = 0.01$, and, with two values of quality factor, $Q = 1$ and $Q = 10$, respectively. Thick solid lines are expectations of $\langle I(t)\rangle$ according to Eq. (4).

$$S = \frac{2^{5/2}}{3(Q^{3/2} + 2Q^{-1/2})}(e^*\omega_J)^{1/2}\bar{I}^{-1/2}. \tag{7}$$

Results (5)–(7) hold also in the overdamped case ($Q < 0.5$). It is interesting to note some general features of S in Eq. (7). The non-Gaussian "strength" increases, in accordance with the central limit theorem, with decreasing $\bar{I}$ (less events recorded). The detector exhibits a memory of events over a time $\sim 2Q/\omega_J$ in the underdamped [$1/(Q\omega_J)$ in the overdamped] case, and, therefore, the skewness attains its maximum value close to the crossover between underdamped and overdamped behavior, $Q \simeq 1$: here the memory of the detector is shortest, and it responds to only a small number $\bar{n}$ of Poisson distributed events through the scatterer. In the example discussed below, $\bar{n} \sim (\bar{I}/e^*)(2Q/\omega_J) \simeq 40$.

Figure 3 shows an example of the simulated (3×10^5 repetitions) current distribution at the time instant $\omega_J t = 40$ (far enough after the initial transient, $\omega_J t \gg 2Q$) for

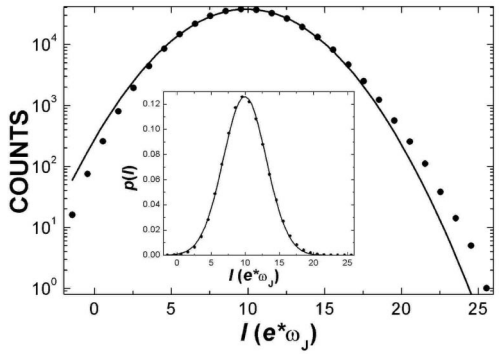

FIG. 3. Simulated current distribution at $\omega_J t = 40$, $Q = 2$, and $\bar{I} = 10e^*\omega_J$. The main frame shows the number of counts (out of 300 000) in solid dots, and the solid line is the best Gaussian fit to it. The inset shows the same results but as the true distribution, = counts/300 000, and on linear scale.

the injected current with $\bar{I} = 10e^*\omega_J$ and for a detector whose $Q = 2$. The main frame with a logarithmic vertical scale shows the number of counts (in solid circles), demonstrating how the simulation differs from the Gaussian fit shown by the solid line. There are more hits at high currents in the simulation as compared to the normally distributed events as one would expect. The same is shown as the true distribution (counts divided by 3×10^5) on a linear scale in the inset. Table I gives a comparison between the simulated values and the theoretical predictions [Eqs. (4)–(6)] of the three lowest moments. The correspondence is satisfactory, although the variance $\langle \delta I^2 \rangle$ falls outside the 1σ uncertainty margin.

Next we make a judgment of whether such a threshold detector provides a viable means to measure FCS. To this end we need to consider the escape rates from the supercurrent state. We assume low temperature T such that thermally activated switching is suppressed. This is the case when $T < \hbar\omega_J/(2\pi k_B)$, which is an easily accessible regime experimentally [10]. The escape rate in the MQT regime in the presence of Gaussian noise has been discussed, e.g., in Ref. [11]. Here, we allow for more general current statistics. Using the standard decay law we find that the probability of escape is given by

$$P = 1 - \exp\left[- \int_{t_0}^{t_0+\Delta t} \Gamma(I(t))dt \right], \tag{8}$$

where Δt is the duration of the current pulse starting at $t = t_0$ over which we monitor escape statistics. Γ is the current dependent escape rate in the MQT process for which one can find explicit expressions that depend on the junction and circuit parameters [12]: $\Gamma = A\exp(-B)$, where $A = \chi\sqrt{\hbar\omega_J \Delta U/(2\pi\hbar)}$ and $B = s\Delta U/(\hbar\omega_J)$. ΔU is the I dependent barrier height, and parameters χ and s are Q dependent. They assume values $\chi = 12\sqrt{6\pi}$ and $s = 36/5$ for large Q. For a pulse with $\Delta t \gg Q/\omega_J$ we may write $\int_{t_0}^{t_0+\Delta t} \Gamma(I(t))dt \simeq \langle\Gamma\rangle\Delta t$, where $\langle\Gamma\rangle \equiv \int_{-\infty}^{+\infty} \Gamma(I)p(I)dI$. Here $p(I)$ is the current distribution approximated, e.g., in Fig. 3. In the scheme of Fig. 1 the average current $\bar{I}$ through the Josephson junction can be generated by any combination of the two (average) currents $\bar{I}_1$ and $\bar{I}_2$ with the constraint $\bar{I} = \bar{I}_1 + \bar{I}_2$. Of particular interest are the cases where $\bar{I}_1$ is either equal to 0 or has positive or negative values of equal magnitude. The difference in the escape characteristics between the latter two cases provides a measure of the asymmetry of $p(I)$ around its mean, the central topic of this Letter. Figure 4

TABLE I. Results.

	Simulation	Theory
$\langle I \rangle$	10.01 ± 0.01	10.00
$\langle \delta I^2 \rangle$	9.91 ± 0.03	10.00
$\langle \delta I^3 \rangle$	4.65 ± 0.22	4.44

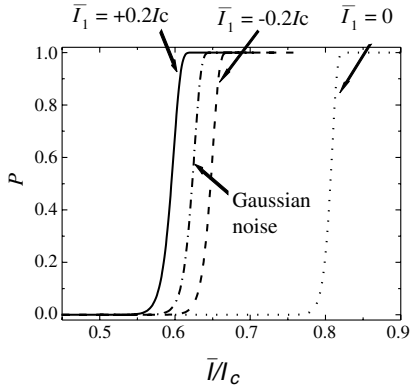

FIG. 4. Escape probability P of a Josephson junction as a function of the average current $\bar{I}$ through the detector under different noise conditions. The shift between the solid and the dashed lines arises from Poisson statistics of charge injection. The dash-dotted line is the escape probability with the corresponding Gaussian noise (same $\langle \delta I^2 \rangle$). Escape in the ideal case of noiseless current is shown by the dotted line.

shows the escape histograms calculated under three such conditions using trapezoidal current pulses of duration $\Delta t = 100\ \mu$s [7,13]. We assume that the detector junction has a critical current $I_C = 1\ \mu$A [$L = \hbar/(2eI_C)$], $C = 0.1$ pF, and other parameters and $p(I)$ are as in Fig. 3. (With these parameters $\Delta t \gg Q/\omega_J$.) We assume pure MQT escape with low dissipation [11,12]. The histograms are plotted as a function of average current $\bar{I}$ through the detector driven by the two injection currents in different proportions. The histogram shown by dotted lines corresponds to no current fluctuations; i.e., all current is driven through the ideal line ($\bar{I}_1 = 0$). The solid line is for the case when current through the scatterer and that through the detector point in the same direction ($|\bar{I}| = |\bar{I}_1| + |\bar{I}_2|$). With our circuit parameters $\bar{I}_1 = +0.2I_C$. The dashed line is for the case when current I_1 points opposite that through the detector ($|\bar{I}| = ||\bar{I}_1| - |\bar{I}_2||$ and $\bar{I}_1 = -0.2I_C$). The average shift of the $\bar{I}_1 = \pm 0.2I_C$ histograms with respect to the dotted line is due to the variance of current, whereas the pronounced shift between the last two is the more interesting effect of non-Gaussian current statistics.

We conclude with a few practical remarks. The scheme presented here is simplified in many ways. First, we do not take into account the (weak) dependence of the plasma frequency (Josephson inductance) on I to keep the discussion more phenomenological and transparent. This is fairly well justified, for example, in the case of Fig. 4, because all the relevant escape currents are smaller than $0.8I_C$, and $\omega_J \propto (1 - I/I_C)^{1/4}$. Second, the escape histograms calculated assume low dissipation, which is not truly the case. The influence of dissipation on the MQT rate through environmental noise can be taken into account by a minor scaling of χ and s parameters [11], and again to keep analysis on the basic level, we omit this since the effect is weak even when $Q = 2$. Third, we assume that the injected charges do not produce current pulses either in the I_2 current line or in the line to the voltage amplifier. This can be realized by large inductance (L_{ext}) in these lines, which in practice means long and narrow wires. If $L_{ext} \gg L$, our argument is justified. Finally, the presented model is based on a classical description of the circuit dynamics: this is a valid starting point in the case of a tunnel junction scatterer whose tunnel resistance $R_T \gg \hbar/e^2$.

I acknowledge very valuable discussions with Dmitri Averin, Frank Hekking, Rosario Fazio, Tero Heikkilä, Antti Niskanen, Pertti Hakonen, and Edouard Sonin.

[1] L. S. Levitov, H. W. Lee, and G. B. Lesovik, J. Math. Phys. (N.Y.) **37**, 4845 (1996).
[2] *Quantum Noise in Mesoscopic Physics*, edited by Yu. V. Nazarov (Kluwer, Dordrecht, 2003).
[3] T. T. Heikkilä and L. Roschier (to be published).
[4] B. Reulet, J. Senzier, and D. E. Prober, Phys. Rev. Lett. **91**, 196601 (2003); B. Reulet, L. Spietz, C. M. Wilson, J. Senzier, and D. E. Prober, cond-mat/0403437.
[5] G. B. Lesovik, JETP Lett. **60**, 820 (1994).
[6] J. Tobiska and Yu. V. Nazarov, Phys. Rev. Lett. **93**, 106801 (2004).
[7] F. Balestro, J. Claudon, J. P. Pekola, and O. Buisson, Phys. Rev. Lett. **91**, 158301 (2003).
[8] Low transmission tunnel junctions follow the Poisson process, a limiting case of the Bernoulli process. Other coherent conductors, ballistic and diffusive ones, were discussed in Ref. [6], where they demonstrated that non-Gaussian fluctuations yield comparable signals to those in tunnel junctions. Our proposed scheme can be used to probe such scatterers as well.
[9] We do not restrict to $e^* = e$, only, because, for example, in normal-superconductor tunnel junctions, the Poisson process is associated with $e^* = 2e$, and also in incoherent Cooper pair ($e^* = 2e$) tunneling noise and FCS play a role.
[10] See, e.g., J. M. Martinis, M. H. Devoret, and J. Clarke, Phys. Rev. B **35**, 4682 (1987), or Ref. [7].
[11] J. M. Martinis and H. Grabert, Phys. Rev. B **38**, 2371 (1988).
[12] A. O. Caldeira and A. J. Leggett, Phys. Rev. Lett. **46**, 211 (1981); Ann. Phys. (N.Y.) **149**, 374 (1983); **153**, 445 (1984).
[13] We thus assume that $\bar{I} = \text{const}$ for $t_0 < t < t_0 + \Delta t$, and that it vanishes otherwise. The transients at the beginning and at the end of the pulse are, however, assumed to be adiabatic. This is the case if the current injection lines are low-pass filtered with cutoff frequency f_C such that (as an example) $f_C^{-1} \sim 1\ \mu\text{s} \gg \omega_J^{-1} \simeq 10$ ps, whereby, on the other hand, the pulses remain nearly rectangular since $\Delta t = 100\ \mu\text{s} \gg f_C^{-1}$.